Title

Impacts of speciation and extinction measured by an evolutionary decay clock

Authors: J. F. Hoyal Cuthill[1,2,3*], N. Guttenberg[2,4,5] and G. E. Budd[6]

Affiliations:

[1]Institute of Analytics and Data Science and School of Life Sciences, University of Essex, Wivenhoe Park, Colchester, CO4 3SQ, UK

[2]Earth-Life Science Institute, Tokyo Institute of Technology, Tokyo, 152-8550, Japan

[3]Department of Earth Sciences, University of Cambridge, Downing Street, Cambridge, CB2 3EQ, UK

[4]Cross Labs, Cross Compass Ltd., 2-9-11-9F Shinkawa, Chuo-ku, Tokyo 104-0033, Japan

[5]GoodAI, Na Petynce, 213/23b, 169 00, Prague, Czech Republic

[6]Department of Earth Sciences, Palaeobiology Programme, Uppsala University, Villavägen 16, SE752 36, Uppsala, Sweden

*Correspondence to: j.hoyal-cuthill@essex.ac.uk

Abstract

The hypothesis that destructive mass extinctions enable creative evolutionary radiations ("creative destruction") is central to classic concepts of macroevolution[1,2]. However, the relative impacts of extinction and radiation on species co-occurrence have not been directly quantitatively compared across the Phanerozoic Eon. Here we use a novel application of machine learning (ML) to generate a spatial embedding (multidimensional ordination) of the temporal co-occurrence structure of the Phanerozoic fossil record, covering 1,273,254 Paleobiology Database occurrences for 171,231 embedded species. This facilitates simultaneous comparison of macroevolutionary disruptions, using measures independent of secular diversity trends. Among the 5% most significant disruption times,

we identify the big five mass extinction events[2], seven additional mass extinctions, two combined mass extinction-radiation events and fifteen "mass radiations". In contrast to narratives emphasising post-extinction radiations[1,3], the proportionally most comparable mass radiations and extinctions (such as the Cambrian explosion and end-Permian mass extinction) are typically decoupled in time, refuting any direct causal relationship between them. We then show that, in addition to extinctions[4], evolutionary radiations themselves cause evolutionary decay (modelled co-occurrence probability and shared fraction of species between times approaching zero), a concept which we describe as "destructive creation". A direct test of the time to over-threshold macroevolutionary decay[4] (shared fraction of species between two times <= 0.1), counted by the "decay-clock", reveals saw-toothed fluctuations around a Phanerozoic mean of 18.6 million years. As the Quaternary Period began at a below-average decay-clock time of eleven million years, modern extinctions further increase life's decay-clock debt.

Main

The destructive effects of extinction, especially mass extinction events, include direct elimination of up to ~75 percent of living species[3], resulting decay of evolutionary and ecological communities[3,4] and potential ecosystem collapse[5]. However, major creative[6] impacts have also been hypothesised via the vacation of ecological niches[4], post-extinction diversification[7], altered evolutionary trajectories[3,8] and shifts in the dominance of particular clades, including our own[3,5,6,9]. We group such latter hypotheses under the concept of evolutionary "creative destruction". In the weak sense, this predicts that extinctions have often enabled subsequent diversifications[1]. In the hard sense, the hypothesis of creative destruction can be expressed as a causative necessity: that major radiations *require* prior mass extinctions[1,3,5,10]. Recently, however, classic narratives of mass extinction, replacement and recovery have been called into question by complicating factors such as significant diversification pre-dating a proposed enabling extinction[11], protracted extinctions[12], and

debates on mass versus background extinction rates and effects[2]. In addition, extinction and radiation may theoretically be more or less decoupled in time[10]. New groups might radiate without a preceding decrease in diversity (pure evolutionary "creation"). On the other hand, biological groups lost in mass extinctions may not be replaced, either immediately or at all, for example due to the temporary[1,2,4] or permanent elimination of the ecological niche they represent (pure evolutionary "destruction"). Furthermore, we propose that the evolutionary radiation of one group may itself cause evolutionary decay (the dilution by origination, or erosion by extinction[4], of pre-existing communities), a concept which we describe, conversely, as "destructive creation". However, the relative evolutionary impacts, balance and timing of radiation and extinction have not previously been quantitatively tested. These fundamental knowledge gaps affect assessments and predictions of recent extinction impacts and recovery potential, which require quantitative baselines from historical diversification and extinction[3].

Machine learning of time structure in the fossil record

Our machine learning (ML) embedding method (Supplementary Computer Code 1, methods summary figure, Extended Data Fig. 1a) allocates every fossil species a location in a multi-dimensional spatial embedding, in which proximity represents the probability of temporal co-occurrence (the probability assigned by the ML model to whether species are observed to co-occur in time, equation 1). This optimises, over the global record of species occurrences, the relative spatial position of each species, such that species which overlapped in time are close together and species that never co-existed are far apart. This enables visualisation of the time structure of species co-occurrences and reveals major disturbances in the history of life. Co-occurrence of fossil species was defined at relatively small time increments of 1 million years, enabling exploitation of the full temporal resolution of raw occurrence data (which aids the detection of evolutionary phenomena[3,13]). Sets of co-existing species are the fundamental constituents of any evolutionary biota, which may persist (to a greater or lesser extent), at one or more taxonomic levels[9,14–16]. A set of co-existing

species is also the maximal set for possible ecological interactions, since co-occurrence in time is necessary (though not in itself sufficient[17]) for ecological interaction. Therefore, temporal co-occurrence probability also provides an evolutionarily (and therefore ecologically) meaningful distance measure between fossil species that facilitates new analyses of the persistence versus decay of co-occurrences. The machine-learnt distances are then related to exhaustively calculated measures of species occurrence across time (shared species fraction between compared times) and proportionate extinction[2] versus origination[18]. In concert, these measures provide new insights into the relative impacts and timing of extinction and radiation, independent of background trends in diversity (computer simulations, Extended Data Fig. 1b-g).

The analyses are based on global fossil occurrences (finds of fossil species from given times and geographic locations) publicly available in the Paleobiology Database (PBDB), including 1,273,254 occurrences for 171,231 species in the complete dataset. After strict data screening to only those occurrences classified to species and phylum level the dataset included 665,590 occurrences for 137,779 species. The dataset covers a broad taxonomic sample of 64 animal, plant and protist phyla and extends from the Neoproterozoic Eon to the recent past, with unbroken Phanerozoic data-coverage from 532 Ma in the Cambrian Period to today (0 Ma).

These analyses permit new quantitative tests of both longstanding and novel hypotheses in macroevolution, including: 1, Simultaneous comparison of the scale and pattern of macroevolutionary disruptions across the Phanerozoic fossil record. 2, Quantitative assessment of the relative balance and timing of mass radiations and extinctions from 580 Ma to the present. 3, Direct tests of the hypothesis of constant evolutionary decay[4] and 4, the corresponding impacts of extinction and radiation on macroevolutionary decay versus persistence.

Time structure of the fossil record

The temporal co-occurrence structure of the fossil record, as represented by our multi-dimensional machine-learnt spatial embedding, was first visualised by using principal component

analysis (PCA) to generate lower dimensional projections from the full 16-dimensional embedding (Fig. 1). The spatial embedding method takes temporal co-occurrence structure, usually exclusively a property of groups of species[13,14,19], and translates it into an optimal embedding location for each individual species. This facilitates simultaneous representation of the pattern of overlaps and separations between species time ranges in the fossil record (the time structure of species co-occurrences). Here, evolutionary restructuring events during the history of life are visible as shifts in species co-occurrence structure in spatial embedding projections to 3D, 2D or 1D (Fig. 1, PCA, explained variance: axis 1, 26%; 2, 15%; 3, 10%). In contrast, a simpler method applying PCA directly to vectors of species time occurrences recovers coarse time structure but not major evolutionary events (Supplementary Computer Code 5). 80% bootstrap data sub-samples (Supplementary Computer Code 6) showed local stability of relative embedding positions across 18 retrained replicates (Extended Data Fig. 2a).

Marked effects on temporal co-occurrence structure are apparent during episodes of both diversification and extinction. For example, the end-Permian mass extinction (the 'great dying') corresponds to a major break-point in co-occurrence among species occurring before and after the boundary between the Paleozoic and Mesozoic eras (red to blue transitions Fig. 1). All our analyses recover this end-Permian mass extinction as the most significant restructuring event in the continuous Phanerozoic fossil record and the most marked break with preceding times (Fig. 2a, Extended Data Fig. 2b-e), as further described below. However, major restructuring events are also identified during episodes of diversification[14].

Balance between radiation and extinction

Attempts to characterise macroevolution have often focussed on mass extinctions and subsequent ecological replacements, including implicit causative hypotheses of "creative destruction" which assume that large-scale radiations require preceding mass extinctions[1,3,5]. However, comparisons of proportionate origination[18] versus extinction[2] at 1 million year increments

through the Phanerozoic Eon (Supplementary Computer Code 2) illustrate that evolutionary "destruction" and "creation" have been almost perfectly balanced, with a full continuum of events between these extremes (Fig. 3, Extended Data Fig. 3). All of the big five mass extinction events previously identified based on drops in raw[2] or subsampled[20] diversity are among the 5% most significant times of evolutionary disruption identified here. However, among the most significant disruption times we additionally identify seven other mass extinctions, fifteen comparable-scale diversifications, which we therefore call the "mass radiations", and two combined mass extinction-radiation events (Fig. 3, Table 1). From either side of this continuum it is therefore possible to identify mirror (or "looking glass") events, which show the most closely reversed proportions of species entering or exiting the fossil record (Fig. 3, Table 1). For example, the most extreme mass radiation is the signal of the Cambrian explosion at 541 Ma, at which 87% of species enter the record and 12% leave. The closest mirror to this is the end-Permian mass extinction, which saw 73% extinction but also 19% origination within a million year window.

This analysis shows that the most comparable mass radiations versus extinctions (e.g. mirror events among the 5% most significant disruption times, Table 1) are in general temporally decoupled, strongly arguing against an immediate causal connection between them. In particular, the proportionately most extreme mass extinctions were, necessarily, not accompanied by a radiation of comparable scope within the same 1 My time window (Table 1). Nor are the mass extinctions generally observed to be closely followed by a mirroring mass radiation (Pearson correlation $r = 0.20$, $p = 0.295$, Shapiro-Wilk $W = 0.934$), which would be predicted by niche vacation and direct replacement for example[1,3,10]. Instead, the events in Phanerozoic history which have created proportionately most diversity (including mass radiations at the beginning of the Cambrian, Carboniferous, Late Ordovician and early Cretaceous) have generally occurred at times that were widely separated from the mass extinction events (Table 1, Extended Data Figure 4). The most extreme of these mass radiations are the Cambrian explosion (from 541 Ma)[18,21], in which species

representing many animal phyla first appear, and the beginning of the Carboniferous Period (358 Ma), in which a signal of major terrestrialisation is evident in both plant and animal speciations (Extended Data Fig. 5). Therefore, the proportionately largest radiations arguably occurred not after ecological niches were vacated by comparable-scale extinctions[1,3,10] but when life exploited new realms of opportunity[10,18,21,22]. One notable exception to this temporal de-coupling of mass extinction and radiation is the end-Permian mass extinction at 252 Ma, which was followed closely[2,18,20] by two significant radiation events at 251 and 247 Ma. Mapping of these mass turnover events, evident from proportionate extinction or origination, onto the visual output from our machine learnt spatial embedding, shows that these are associated with major shifts in species co-occurrence structure (Figs. 1-2, Extended Data Fig. 2c,e).

Macroevolutionary decay

Visualisation of all possible time-to-time distances (Fig. 2) generally shows a trail of high, then decaying, co-occurrence probabilities. This trail extends from a given base time, back to those times before it in which existing species remain comparatively closely located within our multi-dimensional spatial embedding. Its fall-off represents the process of macroevolutionary turnover over which the probability of species co-occurrence falls to a very low level. Across the Phanerozoic, the exhaustively calculated fraction of fossil species shared between any two times (which is closely conceptually related to the co-occurrence probability but here has the additional advantage of non-heuristic value calculation) falls below 0.1 in a mean of 18.6 million years (taxonomically screened species dataset, standard deviation, SD = 9.84, median = 17 My). This decay rate results from the distribution of species occurrence times and ranges, which in aggregate comprise the fossil record (90% ranges <= 19.8 My, median = 6.5 My, additional summary statistics, Extended Data Fig. 6a-b). The fraction of species shared between times falls below 0.5 in a mean of 4.4 My (SD = 3.1), therefore this represents the relative half-life of species occurrences. A lower threshold of 0.05 is reached at a mean of 30.6 My (SD = 14.9). For comparison against the shared fraction, the

probability of species co-occurrence across compared times (calculated from the mean time-to-time embedding distance, Fig. 2) falls below 0.1 in a mean of 30.4 million years for the complete dataset, similarly 32.5 My after strict taxonomic screening. Therefore, on average for a time series, by approximately 19 million years after it starts proportionally very few, to none, of the species that exist will be those that were present at the beginning. Conversely, by this time the existing species will, on average, be entirely new.

Across the Phanerozoic as a whole, this time to over-threshold evolutionary decay fluctuates around an approximately constant mean (Fig. 2). This equilibrium level has been consistently returned to over Phanerozoic history despite secular diversity increases during this period[20] (from which our measures of co-occurrence structure are largely independent, Extended Data Figs. 1b-g, 6b, 7e). Based on constant extinction probability estimates for taxa of different ages, Van Valen predicted that the effective environment[4] (ecological[23] setting) of a given species would tend to deteriorate at a constant rate (the Red Queen hypothesis)[4]. The measures of species co-occurrence calculated here provide a direct estimate of the decay rate of macroevolutionary structure, which we call the "decay-clock". The decay-clock counts the time to over-threshold evolutionary decay, which is here defined as the time (looking back from each base time, Fig. 2b-d) at which the shared fraction of species (or co-occurrence probability) approaches zero (specifically falling to 0.1). As the global set of co-occurring species is the arena within which all ecological interactions must take place, the decay-clock shows how this maximal ecological envelope decays or persists over time. Our results demonstrate that the global Phanerozoic biota has indeed decayed over an equilibrium average of 19 million years (Fig. 2b). However, rather than remaining flat (as might be the expectation from a consideration only of the mean or maximum species range, Fig. 2b), we show that macroevolutionary decay is characterised by dynamic fluctuations around this long-term average as species co-occurrence structure is periodically disturbed then gradually recovers continuity.

At times of major evolutionary disruption during the Phanerozoic (Fig. 3), the normal chains of species co-occurrences have been broken, leading to sudden discontinuities (Figs 1-2). Here, the probability that any existing species co-occurs with species from any preceding time fell to exceptionally low levels at an exceptionally rapid rate (Fig. 2). Most markedly, the great majority of species which have lived at any time from 251 million years ago onwards did not occur before the end-Permian mass extinction, or co-occur with any species which existed in the preceding Palaeozoic Era. Consequently, there was a dramatic increase in the rate of macroevolutionary decay at the end of the Permian Period (Fig. 2c, Extended Data Fig. 6c,d), with a drop to a shared species fraction of 0.1 1 million years after this extinction event (reaching 0.1 before 253 Ma, 19 times faster than the Phanerozoic mean). As time goes on, after each such disturbance event, the decay-clock time can only increase gradually, each My that >10% of a given biota has persisted. This highlights an inherent time-asymmetry in macroevolutionary disturbance and recovery, in that the decay-clock can be rapidly reset but can only count up year by year between disturbances. Comparatively long intervals between major disturbance events are therefore characterised by long-term persistence of evolutionary biotas (the flip-side of evolutionary decay), for example during the Carboniferous and mid-Cretaceous (Fig. 2).

The concept of evolutionary decay was originally formulated in relation to extinctions[4] (conceptual diagram, Extended Data Fig. 7a-c). Extinctions themselves erode a given community by removing original members[3]. However, we show that evolutionary radiations also cause comparable decay by diluting a pre-existing species set, thereby decreasing the co-occurrence probability and fraction of species shared with times preceding a radiation event (Fig. 2, Extended Data Figs. 2b-e, 6e-f, 7a-c). In this sense, mass radiations (Fig. 3, Table 1) can be as destructive as major extinction events. Consequently, the decay-clock has been periodically reset throughout Phanerozoic history by both extinctions and radiations (Fig. 2). While this destructive aspect of evolutionary radiation may initially appear counter-intuitive (since radiations necessarily create new species), recent

biogeography presents numerous examples of the major ecological disruptions that can result from the appearance within an existing community of new invasive species[10]. The analyses conducted here show that disturbances resulting from the evolution of new species have occurred periodically, sometimes on a huge scale, throughout Phanerozoic history (Fig. 2). Those species present at the onset of a mass radiation experienced influxes of new species generating up to 87% of total standing diversity (Fig. 3), with this most extreme example occurring at the Ediacaran-Cambrian transition. Mass radiations have therefore represented disruptions to the prior biota[9,14] at scales comparable to, and in cases exceeding, those of the mass extinctions (Figs. 2-3).

There has been considerable interest in trends in diversity and extinction across Phanerozoic history, including effects of marine versus terrestrial settings[24], biotic[4] versus abiotic[24] extinction-triggers and trends[9,25] and periodicities[26,27] in extinction magnitude (all of which have been subject to scientific debate). Our analysis provides an overview of the relative dynamics of diversity over time, that takes into account all events recorded by the pattern of species occurrences (not solely extinctions or their largest or best known subset). Contrary to some previous results using other measures of diversity or taxonomic levels (e.g. number or percentage of families going extinct within a time interval[25,27,28]), the species-level measures, calculated here, do not show significant declines throughout the Phanerozoic either in the intensity of disruptions to co-occurrence structure or proportional origination or extinction levels (statistics, Extended Data Fig. 7e).

Three major disturbance events in the Eocene epoch of the Paleogene period are particularly relevant to the establishment of the modern ecosystem, including two mass radiations at the start of the epoch and latter Priabonian stage, as well as a mass extinction at the Eocene-Oligocene transition approximately 33 million years ago (Figs. 3-4). Subsequently (while falling outside the 5% most significant times of disturbance), events within the two most recent geological periods of the Neogene and Quaternary show moderate to high levels of disturbance (Fig. 2, detail Extended Data Fig. 7d) with fractional species turnover greater than 30% (within the top 11% of 600 analysed times

and top 30% of 222 times of identified turnover, Extended Data Fig. 3). These events include radiations at approximately 28, 23 and 20 Ma (with originations >= 30%). They also include extinctions (at approximately 15, 5 and 2 Ma) associated with climate change at the end Miocene (5.3 Ma) and Neogene-Quaternary transition (2.58 Ma)[18,29], which, while moderate when compared against the entire scope of Phanerozoic history[2], are formidable from a modern conservation perspective[10] (with species extinction >= 30%). Because macroevolutionary disturbances can reset the decay-clock, these recent extinction events resulted in rapid evolutionary decay (Fig. 2, detail Extended Data Fig. 7d). Consequently, diversity entered the Quaternary period with an already below-average decay-clock time of approximately 11 million years. From that point, the decay-clock would therefore take a minimum of 8 million years without large-scale disturbance to count up to the Phanerozoic mean. Based on the historical processes identified here, modern extinctions and originations are likewise predicted to erase the connections to the past which are measured by the decay-clock. Each modern extinction therefore represents a step towards macroevolutionary decay that further increases the time required to recover to the long-term equilibrium.

References

1. Simpson, G. G. *Tempo and mode in evolution*. (Columbia University Press, 1944).
2. Raup, D. M. The role of extinction in evolution. *PNAS* **91**, 6758–6763 (1994).
3. Hull, P. M., Darroch, S. A. F. & Erwin, D. H. Rarity in mass extinctions and the future of ecosystems. *Nature* **528**, 345–351 (2015).
4. Van Valen, L. A new evolutionary law. *Evolutionary Theory* **1**, 1–30 (1973).
5. Jablonski, D. Extinctions: a paleontological perspective. *Science* **253**, 754–757 (1991).
6. Jablonski, D. Lessons from the past: Evolutionary impacts of mass extinctions. *PNAS* **98**, 5393–5398 (2001).

7. Budd, G. E. & Mann, R. P. History is written by the victors: The effect of the push of the past on the fossil record. *Evolution* **72**, 2276–2291 (2018).
8. Lehman, J. & Miikkulainen, R. Extinction Events Can Accelerate Evolution. *PLOS ONE* **10**, e0132886 (2015).
9. Sepkoski, J. J. A kinetic model of Phanerozoic taxonomic diversity. III. Post-Paleozoic families and mass extinctions. *Paleobiology* **10**, 246–267 (1984).
10. Stroud, J. T. & Losos, J. B. Ecological opportunity and adaptive radiation. *Annual Review of Ecology, Evolution, and Systematics* **47**, (2016).
11. Field, D. J., Benito, J., Chen, A., Jagt, J. W. M. & Ksepka, D. T. Late Cretaceous neornithine from Europe illuminates the origins of crown birds. *Nature* **579**, 397–401 (2020).
12. Wood, R. *et al.* Integrated records of environmental change and evolution challenge the Cambrian Explosion. *Nature Ecology & Evolution* (2019) doi:10.1038/s41559-019-0821-6.
13. Fan, J. *et al.* A high-resolution summary of Cambrian to Early Triassic marine invertebrate biodiversity. *Science* **367**, 272–277 (2020).
14. Muscente, A. D. *et al.* Quantifying ecological impacts of mass extinctions with network analysis of fossil communities. *PNAS* **115**, 5217–5222 (2018).
15. Alroy*, J. Are Sepkoski's evolutionary faunas dynamically coherent? *Evol Ecol Res* **6**, 1–32 (2004).
16. Brett, C. E., Ivany, L. C. & Schopf, K. M. Coordinated stasis: An overview. *Palaeogeography, Palaeoclimatology, Palaeoecology* **127**, 1–20 (1996).
17. Blanchet, F. G., Cazelles, K. & Gravel, D. Co-occurrence is not evidence of ecological interactions. *Ecol Lett* **23**, 1050–1063 (2020).
18. Sepkoski, J. Rates of speciation in the fossil record. *Philosophical Transactions of the Royal Society of London. Series B: Biological Sciences* **353**, 315–326 (1998).

19. Sadler, P. M. Quantitative biostratigraphy—achieving finer resolution in global correlation. *Annu. Rev. Earth Planet. Sci.* **32**, 187–213 (2004).
20. Alroy, J. *et al.* Phanerozoic trends in the global diversity of marine invertebrates. *Science* **321**, 97–100 (2008).
21. Na, L. & Kiessling, W. Diversity partitioning during the Cambrian radiation. *PNAS* **112**, 4702–4706 (2015).
22. Kearsey, T. I. *et al.* The terrestrial landscapes of tetrapod evolution in earliest Carboniferous seasonal wetlands of SE Scotland. *Palaeogeography, Palaeoclimatology, Palaeoecology* **457**, 52–69 (2016).
23. Van Valen, L. V. Adaptive Zones and the Orders of Mammals. *Evolution* **25**, 420–428 (1971).
24. Benton, M. J. The Red Queen and the Court Jester: species diversity and the role of biotic and abiotic factors through time. *Science* **323**, 728–732 (2009).
25. Newman, M. E. J. & Eble, G. J. Decline in extinction rates and scale invariance in the fossil record. *Paleobiology* **25**, 434–439 (1999).
26. Fischer, A. G. & Arthur, M. A. Secular variations in the pelagic realm. (1977).
27. Raup, D. M. & Sepkoski, J. J. Periodicity of extinctions in the geologic past. *Proceedings of the National Academy of Sciences* **81**, 801–805 (1984).
28. Gilinsky, N. L. Volatility and the Phanerozoic decline of background extinction intensity. *Paleobiology* **20**, 445–458 (1994).
29. Pimiento, C. *et al.* The Pliocene marine megafauna extinction and its impact on functional diversity. *Nature ecology & evolution* **1**, 1100–1106 (2017).
30. *A geologic time scale 2004*. vol. 86 (Cambridge University Press, 2004).
31. Ross, R. J., Adler, F. J., Amsden, T. W., Bergstrom, D. & Bergstrom, S. M. The Ordovician System in the United States: correlation chart and explanatory notes. 1–73 (1982).

32. Walker, J. D., Geissman, J. W., Bowring, S. A. & Babcock, L. E. The Geological Society of America geologic time scale. *GSA Bulletin* **125**, 259–272 (2013).
33. Gilinsky, N. L. & Bambach, R. K. Asymmetrical patterns of origination and extinction in higher taxa. *Paleobiology* **13**, 427–445 (1987).
34. Peters, S. E. & McClennen, M. The Paleobiology Database application programming interface. *Paleobiology* **42**, 1–7 (2016).
35. Caswell, B. A. & Frid, C. L. J. Learning from the past: functional ecology of marine benthos during eight million years of aperiodic hypoxia, lessons from the Late Jurassic. *Oikos* **122**, 1687–1699 (2013).
36. Maaten, L. van der & Hinton, G. Visualizing data using t-SNE. *Journal of machine learning research* **9**, 2579–2605 (2008).
37. Mikolov, T., Chen, K., Corrado, G. S. & Dean, J. A. Computing numeric representations of words in a high-dimensional space. (2015).
38. Schroff, F., Kalenichenko, D. & Philbin, J. Facenet: A unified embedding for face recognition and clustering. in *Proceedings of the IEEE conference on computer vision and pattern recognition* 815–823 (2015).
39. Hoyal Cuthill, J. F., Guttenberg, N., Ledger, S., Crowther, R. & Huertas, B. Deep learning on butterfly phenotypes tests evolution's oldest mathematical model. *Sci Adv* **5**, eaaw4967 (2019).
40. Ruder, S. An overview of gradient descent optimization algorithms. *arXiv:1609.04747 [cs]* (2017).
41. Dietterich, T. Overfitting and undercomputing in machine learning. *ACM computing surveys (CSUR)* **27**, 326–327 (1995).
42. Goldberg, Y. & Levy, O. word2vec Explained: deriving Mikolov et al.'s negative-sampling word-embedding method. *arXiv:1402.3722 [cs, stat]* (2014).

43. Heim, N. A. & Peters, S. E. Covariation in macrostratigraphic and macroevolutionary patterns in the marine record of North America. *GSA Bulletin* **123**, 620–630 (2011).
44. Bacaro, G. & Ricotta, C. A spatially explicit measure of beta diversity. *Community Ecology* **8**, 41–46 (2007).

Figure legends

Figure 1. Time structure of the fossil record. a, 1st 3 principal component analysis (PCA) axes from a 16-dimensional machine-learnt spatial embedding where distance represents probability of temporal co-occurrence (equation 1). **b,** 1st 2 PC axes. Points: n = 171,231 fossil species, occurring from 1000-0 Ma (complete dataset). Colours: geological period boundaries e.g. Permian-Triassic, red-blue. **c,** 1st PCA axis after moving-average smoothing, highlighting temporal shifts in co-occurrence structure (vertical movements, either up or down), independent of secular changes in diversity (n = 171,173 species, 600-0 Ma). Vertical lines: 5% most significant times of fractional species turnover (Fig. 3, Table 1); mass extinctions (red), mass radiations (blue), mixed mass extinction-radiations (magenta).

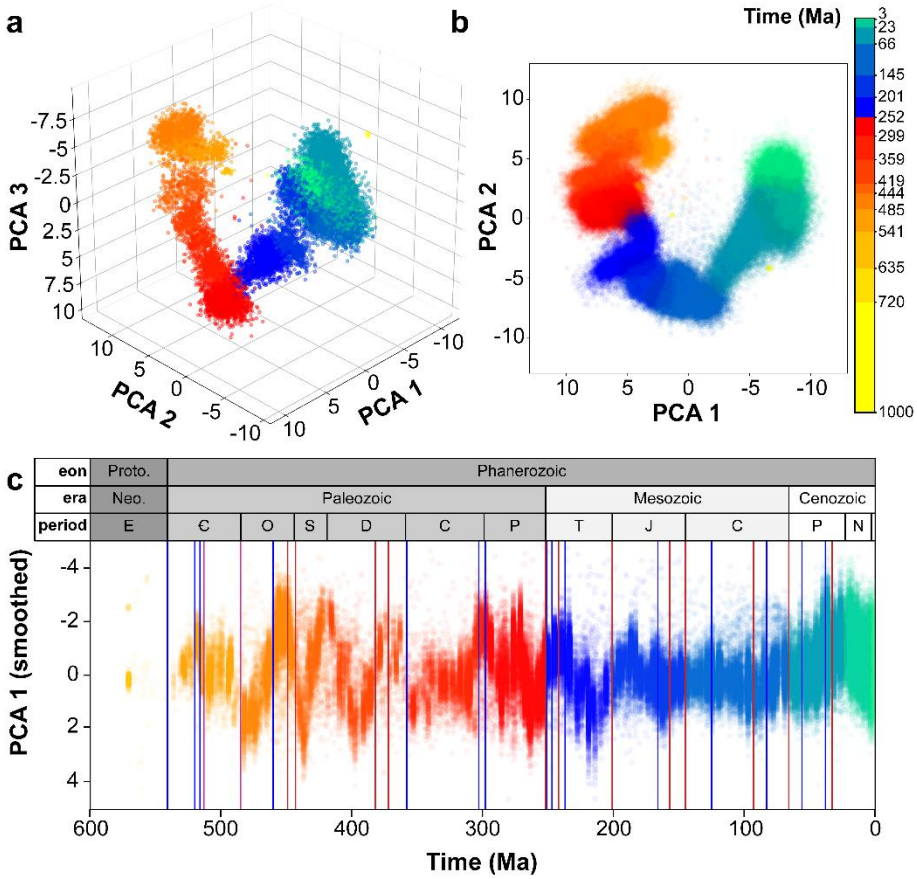

Figure 2. Macroevolutionary decay. a, Heatmap where colour represents mean probability of temporal co-occurrence between species occurring at compared times (complete dataset, all pairwise time comparisons, 1 My increments, 531-0 Ma, n = 532 times) calculated from distances in the ML spatial embedding. **b**, Time to over-threshold evolutionary decay, when the fraction of species shared between a base time and its preceding times falls to 0.1 (taxonomically screened dataset). Horizontal lines indicate mean time to decay (grey) and maximum range among the 90% shortest species ranges (black). Vertical lines indicate 5% most significant mass extinctions (red), mass radiations (blue), mixed mass extinction-radiation events (magenta) (Fig. 3, Extended Data Fig. 4). **c, d**, Examples of major disturbance events at which the rate of evolutionary decay rapidly increased: end-Permian mass extinction (**c**) and subsequent Middle Triassic mass radiation (**d**).

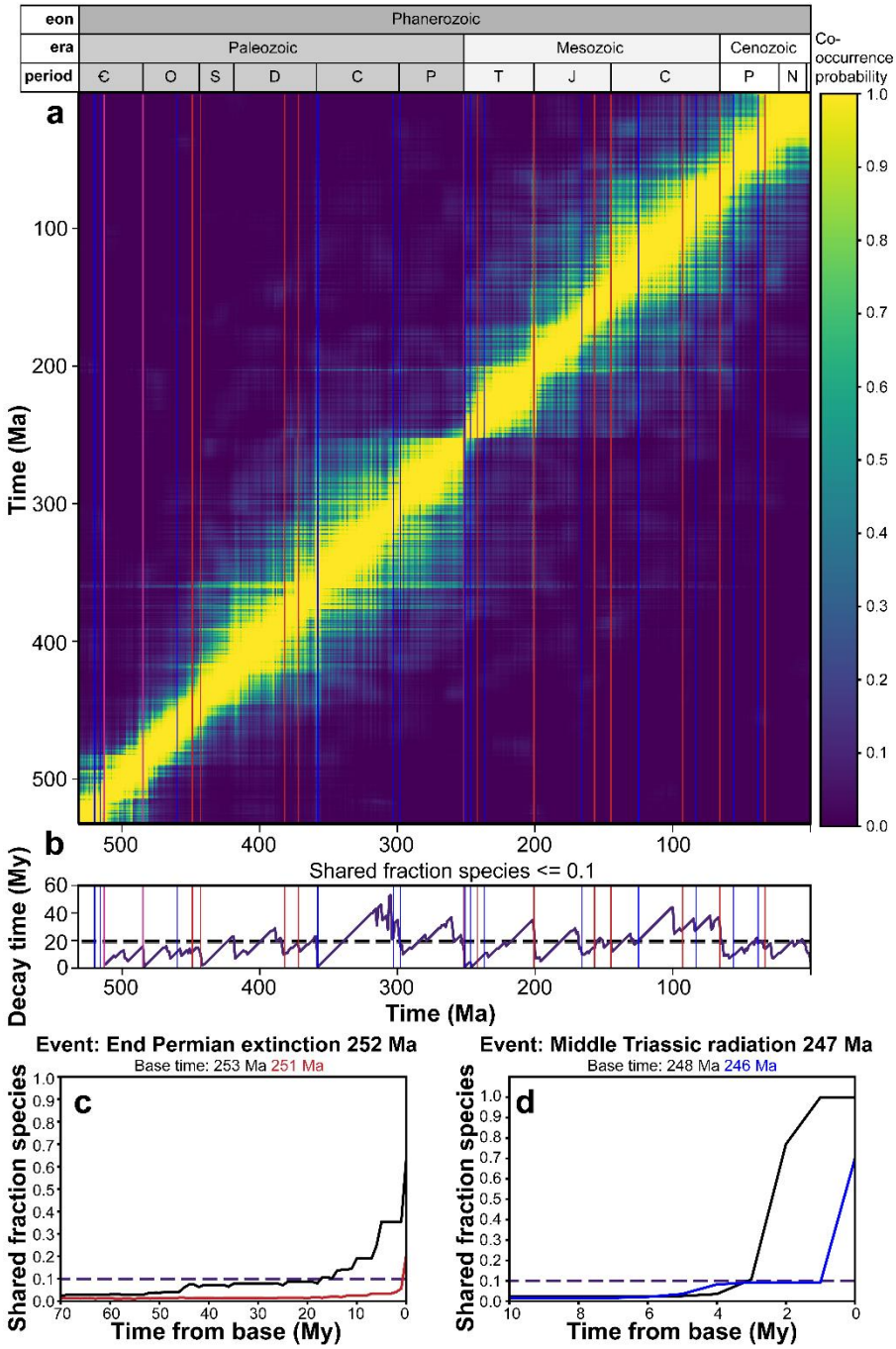

Figure 3. Balance between mass radiation and extinction. Species origination versus extinction, as a proportion of total diversity within the time window, at 1 My increments from 600 to 0 Ma. Data points: n = 222 times at which any species enter or exit the fossil record (taxonomically screened dataset). Labelled times: 30 (5%) most significant event times from 600-0 Ma (corresponding to a > 42% species entry/exit threshold, grey square). Red labels: 'big five' mass extinction events[2].

Colours: magenta, both extinction and origination above threshold (mass extinction-radiation); red, extinction only (mass extinction); blue, origination only (mass radiation).

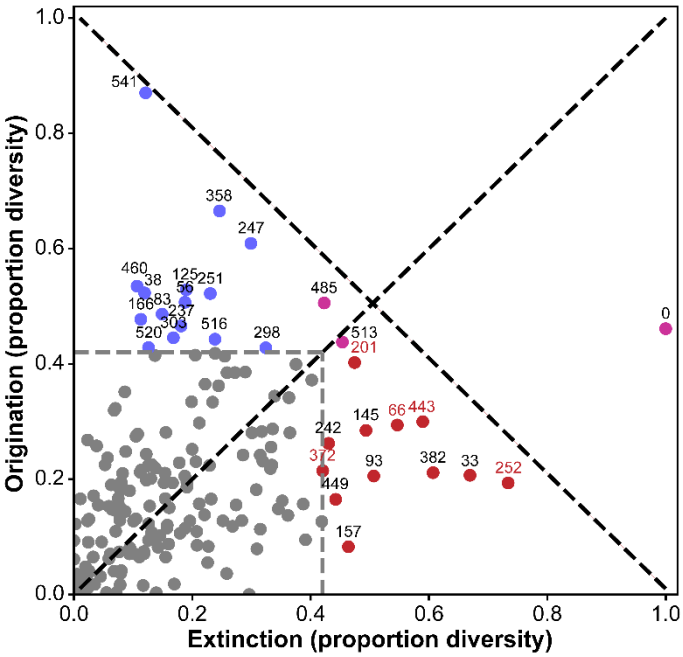

Table 1. Looking glass events in macroevolution. Top 5% fractional species turnover times (n = 29 event times, present 0 Ma excluded) in the Phanerozoic fossil record and their closest mirrors. Mirror events have opposite dominance of species origination versus extinction and closest reversed magnitudes (closest points in mirroring of Fig. 3 across the identity line). Bold ranks: 9 most extreme events (top 5% of 222 identified turnover events). Bold events: 'big five' mass extinction events[2]. Relevant stratigraphic unit names, dates and corresponding references are those used in the PBDB[30*, 31**,32].

Event						Mirror event			
Event rank	**Time (Ma)**	**Classification**	**Event unit**	**Extinctions (%)**	**Originations (%)**	**Time (Ma)**	**Classification**	**Extinctions (%)**	**Originations (%)**
1	541	Mass Radiation	Cambrian start	12	87	252	Mass Extinction	73	19
2	358		Carboniferous start	25	67	33		67	21
3	247		Middle Triassic start	30	61	443		59	30
4	460		Late Ordovician start*	11	53	157		46	8
5	125		Aptian stage start	19	53	93		51	21
6	38		Priabonian stage start	12	52	157		46	8
7	251		Triassic start	23	52	93		51	21
8	56		Eocene start	19	51	93		51	21
9	83		Campanian stage start	15	49	449		44	17
10	166		Callovian stage start	11	48	157		46	8
11	237		Late Triassic start	18	47	449		44	17
12	303		Gzhelian stage start*	17	45	449		44	17
13	516		Nangaoian stage start*	24	44	242		43	26
14	520		Atdabanian stage start*	13	43	449		44	17
15	298		Permian start	32	43	242		43	26
1	485	Mass Extinction-Radiation	Ordovician radiation	42	51	201	Mass Extinction	47	40
2	513		Middle Cambrian start*	45	44	485	Mass Extinction-Radiation	42	51
1	252	Mass Extinction	**End Permian**	73	19	358	Mass Radiation	25	67
2	33		Eocene end	67	21	358		25	67
3	382		Middle Devonian end	61	21	358		25	67
4	443		**End Ordovician**	59	30	247		30	61
5	66		**End Cretaceous**	55	29	247		30	61
6	93		Cenomanian stage end	51	21	56		19	51
7	145		Jurassic end	49	28	251		23	52
8	201		**End Triassic**	47	40	485	Mass Extinction-Radiation	42	51
9	157		Oxfordian stage end	46	8	166	Mass Radiation	11	48
10	449		Blackriveran stage end**	44	17	303		17	45
11	242		Anisian stage end*	43	26	516		24	44
12	372		**Late Devonian**	42	21	516		24	44

Materials and Methods

Palaeobiological data

The raw data for our analyses were temporal occurrences of fossil species publicly recorded in the Paleobiology Database (PBDB). These raw data are time ranges (intervals in the geologic timescale[32]) at which a fossil taxon (e.g. species) was observed to occur. A given taxon (e.g. species) present in the database may therefore be represented by one, or more than one, observed occurrence at one, or more than one, time interval.

Recorded occurrences of fossil species, from the Neoproterozoic to the present, were downloaded from the PBDB using the temporal overlap interval of 1000-0 Ma, with all default output plus taxonomic classification. Analyses were conducted at the fundamental taxonomic level of species to avoid the potential for complicating factors of taxonomic occupancy which may result from the use of higher taxonomic ranks[24,28,33]. PBDB data were therefore downloaded and analysed at two levels of resolution of the taxonomic classification [34]. 1. A taxonomically more inclusive dataset which used unique species names as the IDs for analyses but with PBDB taxonomic resolution set to genus. This allows the inclusion of some fossil occurrence records which are only

classified to the level of genus (e.g. an identified name such as *Acaste sp.*). This gave a total of 1273254 fossil occurrences for 171231 species. 2. A taxonomically more exclusive dataset screened to include only occurrences with an accepted name classified to species rank and with a specified phylum name. This gave a total of 665590 fossil occurrences for 137779 species. More relaxed taxonomic restrictions therefore resulted in 48% more fossil occurrence data for machine learning whereas more strict taxonomic restrictions ensure uniform classification to species and phylum level. Principal results were then compared between the two datasets to determine any effects from these different data-screening protocols. This comparison showed that the main results were similar for the two datasets. Specifically, the rank orders of the magnitude of evolutionary disruptions at one million year intervals were shown to be significantly correlated between the two alternative datasets (Spearman's rank order correlation: fraction of shared occurrences $r = 0.3755$, $p = 2.9752 \times 10^{-19}$; embedding distances $r = 0.0960$, $p = 0.0268$). The top 20% times of evolutionary restructuring identified were also found to have an overlap across the two datasets of 75% for the ML spatial embedding method and 92% for fractional turnover. Therefore, results from both datasets are reported in the main text, with ML visualisations in the main figures showing the complete dataset while additional results, for example shared fractions of strictly taxonomically screened species, are reported in the text and Extended Data figures.

We note that we have not attempted to further process the PBDB raw data in order to correct for any dating uncertainties or preservation bias (see e.g. [29]). Future work, for example, focusing on specific events, might consider incorporating additional data processing steps. However, the events which we identify can be verified against previously recovered patterns of extinction and radiation[2,20,29], suggesting that at the level of our analysis any data inconsistencies have not been sufficient to obscure events of evolutionary interest.

For comparison with the new metrics generated in this study, standard diversity statistics were calculated using the PBDB Navigator. These were the number of genera and families sampled in geological stage time bins.

Machine learning

A new machine learning (ML) spatial embedding method was applied to the raw data of recorded occurrences of 171,231 fossil species in time (ML methods summary figure, Extended Data Fig. 1a). Geographic coordinates of fossil finds, which are also present in the PBDB, were not used in our machine learning method. Our ML method embeds fossil species within a multi-dimensional space (with 16 dimensions) in which inter-species distance represents their probability of temporal co-occurrence (definition, equation 1, below). Co-occurrence for a given pair of fossil species was identified based on temporally overlapping observed occurrences, a standard criterion for co-existence in time[19]. This method thereby takes high-dimensional data (the temporal occurrences of species in the fossil record) and projects it into a low dimensional space that aims to preserve key aspects of that high-dimensional data (specifically the probability of species co-occurrence). Our method falls within a wider class of machine learning embedding methods. Existing machine learning embedding methods include, for example, non-metric multi-dimensional scaling[35], T-distributed Stochastic Neighbor Embedding (t-SNE)[36], the word2vec[37] algorithm that embeds words (in that case in a vector space) and triplet-trained neural networks[38,39]. ML embedding methods may use a variety of machine learning optimisation methods (e.g. here, gradient descent[40]) and specific optimisation functions (here, co-occurrence probability) to place (ordinate) points (e.g. here, representing fossil species) within a multi-dimensional space. Some such embedding methods may additionally be linked with neural network methods and/or data classification steps (e.g. triplet networks[38,39]). However, we note that this is not necessarily the case and the specific method used here is not a neural network method, nor does it involve data classification, or the learning of a trained model which aims to generalise to new data (and may therefore be subject to associated

methodological problems such as model overfitting on the training dataset[41]). Rather, the specific aim of the ML method used here is solely to embed all training data according to the specific optimisation function used (co-occurrence probability). Therefore, the meaning of proximity within our embedding is easily interpretable (as co-occurrence probability) and comparable to exhaustively calculated measures (see brute-force methods below). This is in contrast to some other multidimensional ordination methods, including machine learning methods for example the word2vec algorithm[42], in which the reason for proximity within a constructed space may be difficult to interpret.

The dimensionality of the embedding space (16 dimensions) was arbitrarily chosen in order to project the high dimensional raw data to a comparatively low number of dimensions (a basic aim of dimensionality reduction techniques), while allowing a sufficiently large number of dimensions for the capture of biologically interesting structure in the data.

The machine learnt spatial embedding was generated using a Python program (Supplementary Computer Code 1) implementing the following procedure. Each fossil species (which can have multiple observed occurrences in the database) will be given a 16-dimensional embedding x (which is randomly initialised). We train the embedding over 50,000 training iterations (epochs). Within each training epoch, we train the embedding via gradient descent on a succession of batches (a method used in many current machine learning applications to optimise model parameter values[40]). Each batch consists of 20,000 examples. An example is constructed by first picking a random time window. A random time window is selected rather than a random fossil occurrence because randomising by time window normalises for variations in diversity over time. After a time window has been selected, a random occurrence is picked (whose species has embedding x_1) from that time window. We then randomly select whether this example will be a co-occurrence (or non-co-occurrence), with 50% probability. If a co-occurrence has been selected, we select another random occurrence from that time window (whose species has embedding x_2). If a co-occurrence has

not been selected, we pick another random time window, pick a random occurrence from that time window and ensure that it does not co-occur with x_1. We then calculate the Euclidean distance (d) between x_1 and x_2 and interpret that as a probabilistic prediction of co-occurrence:

$$p(x_1, x_2) = sigmoid\big(a - d(x_1, x_2)\big) =$$

$$p(x_1, x_2) = 1/\left(1 + exp\left(-\big(a - d(x_1, x_2)\big)\right)\right) \quad (1)$$

Where a is a learned parameter of the model, observed during machine learning to be 11.994 for the complete dataset (and 12.5998 for the taxonomically screened dataset).

The learnt parameter a can then be entered into equation 1 to convert a learnt embedding distance d to a corresponding co-occurrence probability.

We train the embeddings and the parameter a to minimise the binary cross entropy:

$$L = E\big[-y\ log\big(p(x_1, x_2)\big) - (1 - y) log\big(1 - p(x_1, x_2)\big)\big] \quad (2)$$

Where p is the probability assigned by the model that the two given species co-occur, and y is the ground truth label (1 when the species co-occur and 0 when they do not).

We used the Adam optimiser with a learning rate of 10^-2 for 50,000 batches.

The length of the ML training time (measured in number of training epochs) for each dataset (real or simulated) was assessed visually and statistically using visualisation tools provided in the supplementary computer code (1-3). These tools allow visualisation of the training error as training proceeds, PCA visualisation of the output embedding and statistical assessment (by visualisation and Pearson correlation) of behaviour of the embedding under simulated secular increases in diversity (linear or exponential).

Comparison of machine learnt spatial embedding to pre-existing methods

This method of ML spatial embedding has some commonalities with previous methods for analysing biological abundance, diversity and temporal co-occurrence, including co-occurrence diversity assessment[13,19] and network analysis[14] (e.g. utilisation of species co-occurrence information) as well as non-metric multi-dimensional scaling[35] (e.g. representation of inter-species

variation within multi-dimensional spaces) but has additional advantages for evolutionary analyses over time. These methodological advantages include: 1. The meaning of inter-taxon distances (probability of species co-occurrence). 2. Consequent opportunities to perform new quantitative tests of macroevolutionary hypotheses. 3. Provision of human-readable data visualisations, facilitating new data-driven insights. 4. Robustness to potential problems of data sampling, crucially including secular variations in fossil preservation potential through time (which show complex relationships with palaeo-diversity that may impact detection or interpretation of evolutionary trends[43]). 5. Capacity to analyse macroevolutionary structure across continuous time series at any specified time increment (e.g. 1 million years). This is in contrast, for example, to standard within-bin diversity counting in comparatively large, discrete time bins (e.g. geological stages which are in the order of tens of millions of years), where increasing bin size is known to impact detection of evolutionary phenomena[13].

Comparison of machine learnt spatial embedding to alternative methods

For comparison to the ML embedding method (described above), a simpler method was implemented (Supplementary Computer Code 5) which applied principal component analysis directly to vectors of the times at which fossil species were observed to occur. This method first takes the raw fossil occurrence data and encodes this as an array of time vectors. Here, each species has one vector of times at which it is recorded to occur (1) or not occur (0) according to the raw observed occurrences. The method then applies a principal component analysis directly to these time vectors so that each fossil species is placed into a PCA projection with 16 components (comparable with our main ML embedding method which uses 16 dimensions for the embedding space). Graphical output and code to generate this is provided as Supplementary Computer Code 5.

Validation of machine learnt fossil embeddings

The measures of macroevolutionary disruption used in this study were designed to be independent of background trends in diversity (which have themselves been extensively investigated

using other methods such as raw diversity analysis[2] and diversity subsampling[20]). The measures used here are therefore normalised for diversity. Diversity normalisation is performed for the exhaustively calculated shared fraction of species between times by using overall diversity as the denominator (see methods section below for further details). Diversity normalisation was also incorporated into the ML spatial embedding method, for example by initially sampling data from times rather than species to avoid excessive weight from high diversity times. However, variation in diversity through time might potentially have unforeseen impacts on the machine learning process and outputs, which are in general highly-data driven. Therefore, in order to validate our methods of machine learning for further evolutionary analyses, we used computer simulations to test the sensitivity of the generated measures to changes in co-occurrence structure versus secular variation in diversity (Supplementary Computer Code 3). We show, using computer simulated data with a known distribution (linear or exponential diversity increase, Extended data Fig. 1b-g), that co-occurrence-based spatial embedding allows the generation of comparative measures which are sensitive to shifts in species co-occurrence but are comparatively unaffected by background trends in diversity (which could themselves occur either due to genuine changes in biodiversity or sampling variation). Specifically, given appropriate ML training time, Pearson correlation indicated no significant correlation between a simulated linear diversity increase and the mean embedding distance between species simulated at successive times ($r = 0.1311$, $p = 0.1936$, Extended Data Fig. 1b-d). A simulated exponential diversity increase produced a weak, though significant, negative trend across successive times ($r = -0.2761$, $p = 7.58E-05$, Extended Data Fig. 1e-g), which can be removed by subtraction of the mean embedding path.

Additional exhaustive calculations of the shared fraction of fossil species between time windows facilitated further validation of, and comparison with, the machine-learnt spatial embeddings (Extended Data Fig. 2b-e), as well as additional evolutionary analyses. Bootstrap analyses (Supplementary Computer Code 6, details below) were used to test whether the ML

methods were methodologically and statistically robust across multiple subsamples of the fossil occurrence dataset (given its size and properties).

Brute-force co-occurrence computations

For comparison with the ML spatial embedding distances, measures of proportionate species co-occurrence between times were calculated using a brute-force algorithm (Supplementary Computer Code 2), implementing the following procedure. For each time t_1 make an array of species occurrences at that time t_1. In this case, a given species is considered present at a given time t if t is within the time range of fossil occurrences of that species observed in the database ($t \geq t_{min}$ and $t \leq t_{max}$, where t_{min} is the minimum observed age of occurrence of the species and t_{max} is the maximum). For the subsequent time t_2 make an array of species occurrences. Calculate the fraction of occurrences that are shared between t_1 and t_2 (shared fraction = intersection/union). The fraction of species that were different was then calculated as the fractional symmetric difference = symmetric difference/union or 1 – shared fraction. If two compared times have exactly the same set of species existing, the shared fraction of species will equal 1. If either originations or extinctions occur, causing sets of species to differ between two compared times, the shared fraction of species between these times will fall. If the sets of species occurring at two compared times are entirely different, the shared fraction of species between times will equal zero.

The fraction of fossil species shared between any two times is closely conceptually related to the co-occurrence probability: both measure the extent and pattern of temporal co-occurrence (between times or between species across time, respectively) but they provide complementary advantages, respectively for the simultaneous visualisation of co-occurrence structure (spatial embedding) versus exhaustive calculation and simplicity of interpretation (shared fractions).

Drill plots and turnover event thresholding

Proportions of species originating versus going extinct at 1 My time increments were calculated and plotted (Fig. 3, Extended Data Fig. 4) using a Python program (Supplementary

Computer Code 4). We present a new type of plot which we call “drill plots” (Extended Data Figure 4) for focal times. These compare stratigraphic ranges of all species occurring within a 1 My time window after the focal time, vertically sorted into originations, extinctions and crossing ranges. Comparisons of event types in these analyses use threshold-based classification into three types: mass extinctions, mass radiations and mixed mass extinction-radiations. To classify events, first the analyses identify all turnover times, at which there are any speciations or extinctions observed in the dataset, within 1 My (<= 0.99 My) of the considered time (Supplementary Computer Code 4). We then calculate the proportions of the occurring species, within this time window, which are originating or going extinct. Each turnover event is then classified as to whether a selected threshold is exceeded by the proportion of extinctions only (in which case it is therefore classified as a mass extinction), radiations only (classified as a mass radiation) or both extinctions and radiations (it is classified as a mixed mass extinction-radiation).

The identification of turnover events in these analyses is, therefore, invariant to the entry/exit threshold used. What can potentially change with an increased threshold is the classification of these events as either a mass extinction, mass radiation or a mixed event. Figures 3 and Extended Data Fig. 4 use a species entry/exit threshold of 42% which was selected in order to highlight the most extreme 5% of turnover times, defined as the top 5% of the 600 times included in this analysis. 5% of the 600 included times equals 30 and the corresponding species entry/exit threshold of 42% is required to return 30 most extreme fractional turnover times. For comparison, Extended Data Fig. 3 shows a lower species entry/exit threshold of 30% which highlights a greater number of turnover times. This 30% threshold was selected as notable based on observation of the data, as this is the level above which all observed turnover events involved both extinction and origination. Choosing a higher entry/exit threshold (e.g. >42%) for included times corresponds to reading off higher extinction/origination percentages from Fig. 3 to restrict consideration to a smaller number of turnover times. For example, another interesting threshold is the top 5% of the 222 identified times

of turnover (out of 600 total times included in this analysis). This equals 11 times, which requires a 53% entry/exit threshold and returns the 10 most extreme times shown on Fig. 3 (with event classification unchanged except for 0 Ma, which does not pass the 53% entry threshold). A 52% entry/exit threshold returns the 13 most extreme times shown on Fig. 3.

"Mirror" events of macroevolutionary restructuring (which we also refer to, in reference to the Red Queen hypothesis[4], as "looking glass" events) were identified, among the events classified using the extinction/origination threshold procedure described above. First, those events with % origination > % extinction were mirrored over the identity line (e.g. on Fig. 3, where % extinction = % origination), by temporarily swapping the x and y axes. The closest mirror events were then identified as those events from opposite halves of the original distribution which had the lowest Euclidean distance after mirroring. These mirror events are, therefore, those which are most comparable in scale but with opposite dominance of radiation versus extinction.

Comparison of brute-force co-occurrence measures to pre-existing methods

The shared fraction of fossil species between compared times (shared fraction = intersection(t1,t2)/union(t1,t2)) can be conceptually related (Extended Data Fig. 7a-c) to the fraction of surviving species (survivor fraction = intersection(t1,t2)/t1), a core concept of standard survivor analyses e.g[4]. The main advantage, for the purposes of this study, of the co-occurrence measures used here (e.g. shared species fraction) is that these measures pick up the effect of any new species originations that have occurred e.g. by time t2. This facilitates the comparison of the parallel effects of extinction and radiation within a unified measurement framework. It also facilitates time-symmetric comparisons e.g. to measure the drop-off in shared fraction of species looking back in time from a given start time or event (Fig. 2c,d). More broadly, the shared species fraction between times also links mathematically to the ecological concept of spatial beta diversity (with beta diversity measures usually considering variation in species composition between spatial samples[44]).

Decay-clock calculations

The time-to-time average species co-occurrence probabilities from the ML analyses and exhaustively calculated fractions of species shared between times were each used to calculate the time to over-threshold decay in species co-occurrence (Supplementary Computer Code 2). For the time range in which there was continuous occurrence data in the datasets (0-532 Ma), this time to evolutionary decay was calculated for each base time, at 1 My increments, looking backwards in time, as follows. First, for each base time, a time series was considered which included all greater times within the total time range for this analysis (e.g. for base time 252 Ma, the considered time series would be 253-532 Ma). Then, the values of the ML co-occurrence probability and fraction of shared species were extracted that compared the given base time to each time in the compared time series. The time taken, along the given time series, for co-occurrence to decay to the threshold value was then recorded. This is counted as the time vector position such that a decay-clock time of 1 means that over-threshold decay has occurred after 1 and within 2 million years. The mean of this decay value was then reported (as the average decay-clock time) across the considered times (0-532 Ma). A number of thresholds were used in this calculation. The main analyses use a decay threshold of 0.1, corresponding to <=10% species shared between considered times. This threshold value of 0.1 was selected because it is a low-level cut-off that remains comparatively representative of species in aggregate (and so will not be driven, for example, by long-lived singleton species as a cut-off of zero might be). For comparison, a threshold of 0.5 was also used, which represents a half-life for species co-occurrence, as well as a lower threshold of 0.05.

To give a worked example of the decay-clock calculation, consider base time 251 Ma (immediately after the end-Permian mass extinction at approximately 252 Ma). For the next few compared times, the fractions of species shared with the base time 251 Ma are for 251 Ma (identity), 1; 252 Ma, 0.21; 253 Ma, 0.06. For a threshold of 0.1, the decay-clock time for 251 Ma is therefore reported as 1 million years since by 253 Ma (i.e. within 2 My years) fewer than 10% of species are shared with 251 Ma.

Geographic range of the analyses

Our analyses use all global fossil occurrences recorded in the PBDB and evaluate temporal co-occurrence only (equation 1). While it would be theoretically possible to extend our ML method to consider geographic locations (within an extended definition of co-occurrence), consideration of time alone has a number of advantages in the context of the present study. First, the examination of patterns of decay in co-occurrence through time has not previously been investigated, whereas ecological patterns in spatial structure have been extensively studied e.g.[21]. Second, by defining co-occurrence based solely on time (and not geographic location) we retain a close conceptual connection between our new ML distance measures and exhaustively calculated statistics on the proportion of species shared across times (as described above), which aids validation and interpretation of the machine learning. Third, by focussing purely on time there is an additional mathematical connection from these new statistics (machine learnt and exhaustively calculated) to fundamental measures of species survival (as described above and shown in Extended Data Fig. 7a-c).

Bootstrap analyses

To test whether the ML methods were methodologically and statistically robust across subsamples of the fossil occurrence dataset a bootstrap procedure was implemented (Supplementary Computer Code 6). The ML embedding analysis was repeated over 18 bootstrap (technical) replicates (with an embedding run-time of 3 days on a GPU computer cluster), each sampling 80% of the 171,231 species from the complete dataset. In order to analyse the stability of the embeddings across ML retraining on these bootstrap data samples, sixty reference fossils were randomly selected for comparison of embedding positions across the bootstrap replicates. These reference fossils were organised into triplets, each of which contained 3 members designated A, B and C. The distances in each learnt embedding between fossils A,B and A,C within each triplet were then compared across bootstrap replicates, using the mean differences and ratios between these distances and their standard

deviations. In order to select reference fossils, 20 reference times were first randomly sampled from the total range of times (at 1 My increments) at which fossils were observed to occur in the complete dataset. Reference fossils were sampled such that all 3 members of a given triplet were observed to occur within 30 My of a given reference time. This sampling process was used in order to ensure that compared fossils within a triplet occurred, relative to each other, within the time range over which the main analyses indicated an average co-occurrence probability above zero (with mean decay to co-occurrence probability <=0.1 observed by 30 My for the complete dataset). This is the approximate time range (average observed for the complete dataset) over which we expect embedding distances to be comparatively tightly constrained by observed co-occurrences.

Statistical and visualisation analyses

Further visualisations and statistical analyses were produced using the ML embedding distances and exhaustively calculated measures of species co-occurrence. Embedding distances and shared species fractions were compared between successive times at 1 My increments for the time interval over which there was continuous data coverage within the fossil occurrence dataset (from 532 Ma, with numbers of species per time window of 5 My for the complete dataset and 1 My for the strictly taxonomically screened dataset). Time-to-time comparisons were conducted for all possible pairwise combinations of time windows of 1 My duration. Here, as above, the occurrence time for each species was summarised as the time-range mid-point across observed occurrences in the database.

Acknowledgements. This research was supported by funding from an IADS Research Fellowship (J.F.H.C.), EON Research Fellowship (J.F.H.C.) at the Tokyo Institute of Technology (supported by a grant from the John Templeton Foundation), Earth-Life Science Institute Research Interactions Committee Visitor Fund (N.G. and J.F.H.C.) and Swedish Research Council (VR grant no. 2015-04726, G.E.B.). Thanks to S. Newman and L. Schalkwyk for computing time and support. Thanks to

S. Conway Morris, as well as E. Mitchell and one additional anonymous reviewer, for highly constructive comments on the manuscript.

Author contributions. J.F.H.C., N.G and G.E.B. designed research, N.G. and J.F.H.C. wrote computer code and performed analyses, J.F.H.C. wrote the paper with input from all authors.

Competing interests. The authors declare no competing interests.

Materials & Correspondence should be addressed to J.F.H.C. j.hoyal-cuthill@essex.ac.uk.

Code and data availability statement

Custom computer code is provided as supplementary material files 1-6. Additional data is provided as Extended Data Figures 1-7. Raw data is publicly available in the Paleobiology Database at https://paleobiodb.org. Additional source data for figures 1-3 is provided in Dryad data repository at https://doi.org/10.5061/dryad.b8gtht79t.

Extended Data legends

Extended Data Figure 1. a, Graphical summary of the machine learning method. b-g, Computer simulations of secular variation in diversity, testing effects on measures of co-occurrence structure used in this study. b-d, Linear and **e-g,** exponential diversity increases (Supplementary Computer Code 3). **b, e,** Heatmaps visualising the machine learnt spatial embedding distance between mean species locations at different times: yellow, closest; purple, farthest. **c, f,** Plot of embedding distances between successive times. **d, g,** Plot of first two principal component axes from the 16-dimensional spatial embedding. ML training times were 3000 training epochs.

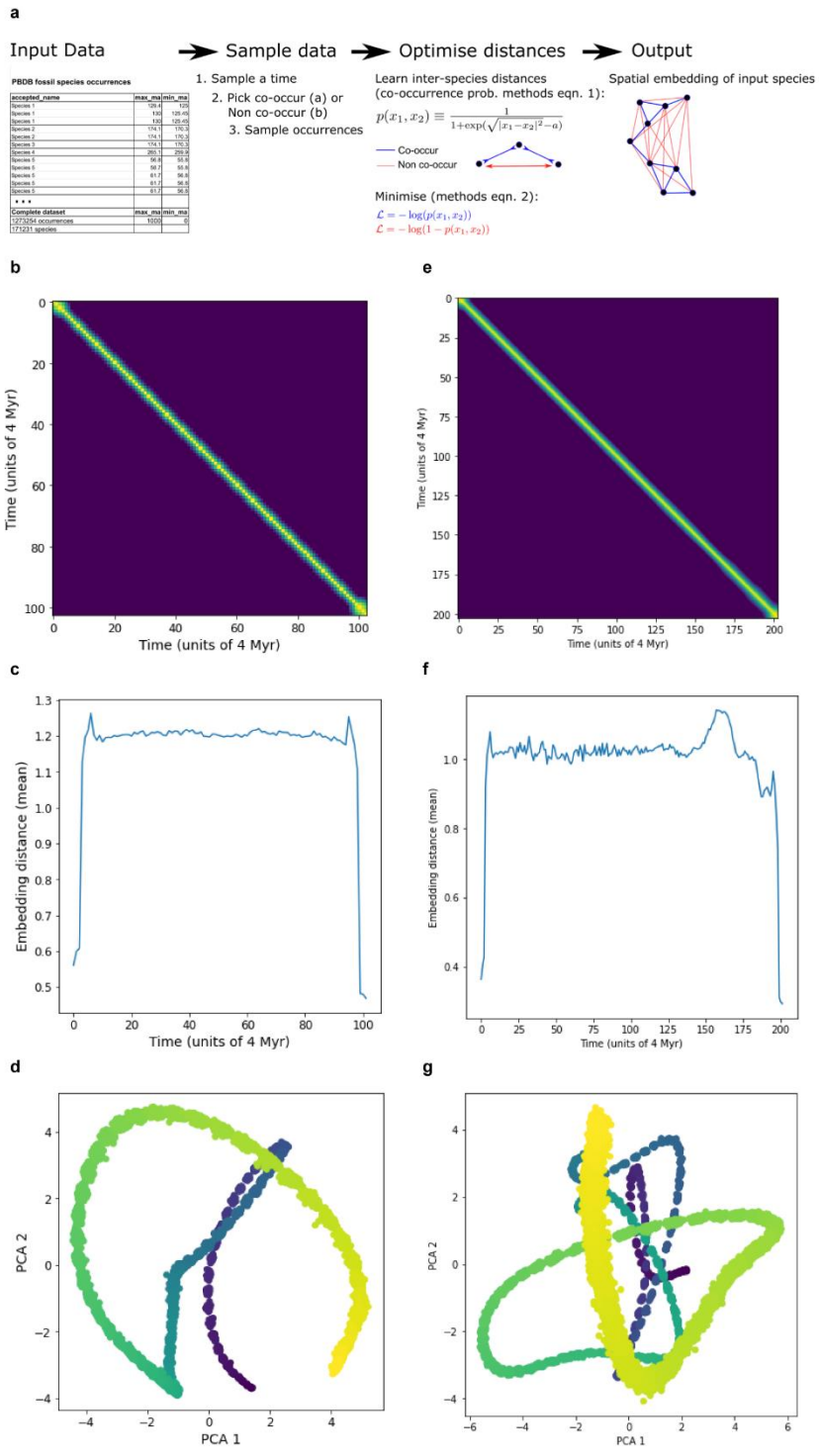
a
Input Data
Sample data
Optimise distances
Output
PBDB fossil species occurrences
1. Sample a time
2. Pick co-occur (a) or Non co-occur (b)
3. Sample occurrences
Learn inter-species distances (co-occurrence prob. methods eqn. 1):
$p(x_1, x_2) \equiv \frac{1}{1+\exp(\sqrt{|x_1-x_2|^2}-a)}$
Co-occur
Non co-occur
Minimise (methods eqn. 2):
$\mathcal{L} = -\log(p(x_1, x_2))$
$\mathcal{L} = -\log(1-p(x_1, x_2))$
Spatial embedding of input species
b
Time (units of 4 Myr)
Time (units of 4 Myr)
e
Time (units of 4 Myr)
Time (units of 4 Myr)
c
Embedding distance (mean)
Time (units of 4 Myr)
f
Embedding distance (mean)
Time (units of 4 Myr)
d
PCA 2
PCA 1
g
PCA 2
PCA 1

Extended Data Figure 2. a, Bootstrap data-resampling results. b-e, Shared fraction of species between successive times (b, d) versus mean embedding distance (c, e). a, Differences in embedding distances for 60 reference fossils, compared within 20 A, B, C triplets over 18 technical replicates of bootstrap data re-sampling and ML embedding training. Error bars show standard deviation of the distance absolute(A-B) - absolute(A-C): mean 0.77. We expect the embedding distances to be comparatively stable within the time range over which co-occurrence probability is within the evolutionary decay range (observed to be mean 30 My for co-occurrence probability to reach 0.1 in the complete dataset). **b, d** Fraction of species which are shared between successive times, calculated exhaustively from raw species time ranges (histogram, Extended Data Fig. 6a). **c, e** the distance in the ML spatial embedding between mean species locations at successive times. Compared times are at increments of 1 My. **b, c,** Complete fossil occurrence dataset. **d, e,** Taxonomically screened dataset. Vertical lines indicate the 5% most significant times of fractional species turnover (Fig. 3, Extended Data Fig. 4): mass extinctions (red), mass radiations (blue), mixed mass extinction-radiations (magenta).

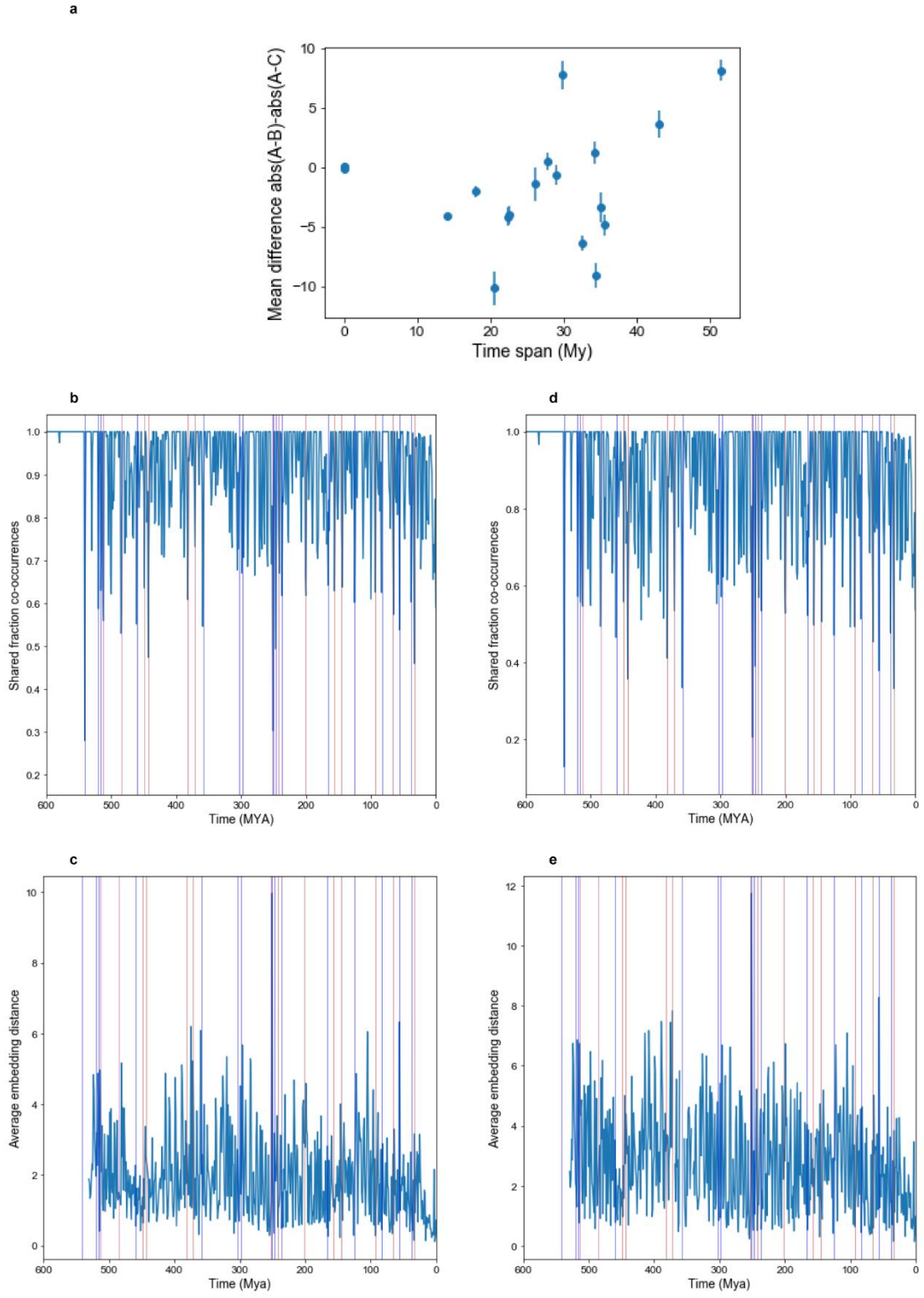
a
Mean difference abs(A-B)-abs(A-C)
Time span (My)
b
Shared fraction co-occurrences
Time (MYA)
d
Shared fraction co-occurrences
Time (MYA)
c
Average embedding distance
Time (Mya)
e
Average embedding distance
Time (Mya)

Extended Data Figure 3. Proportions of species originating versus going extinct. 1 My increments from 600 to 0 Ma with a threshold of 30% species entry/exit threshold, grey square. This threshold highlights the top 66 times of turnover from 222 total turnover times identified among 600 times included in the analysis. Colours as for Fig. 3.

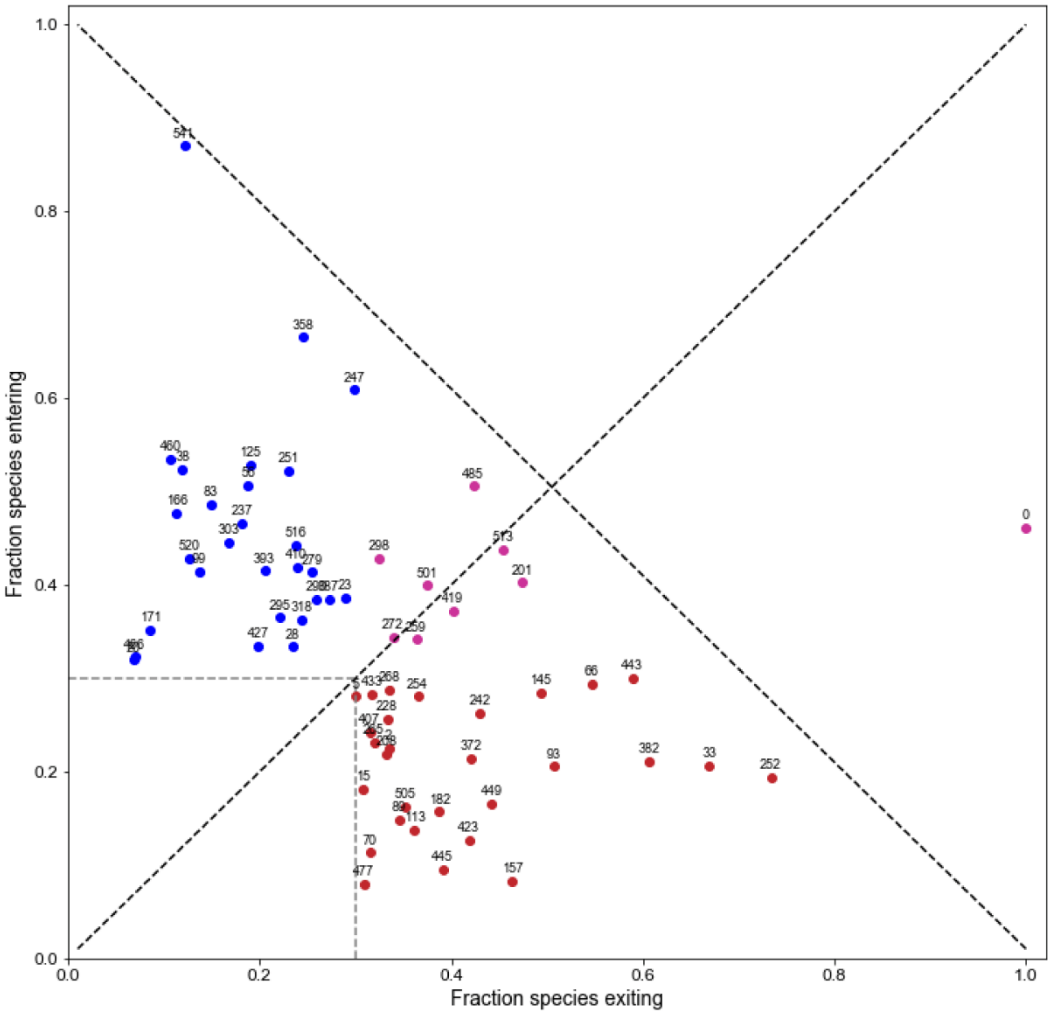
Fraction species entering
Fraction species exiting
0.0
0.2
0.4
0.6
0.8
1.0
541
358
247
460
38
125
251
485
166
83
237
303
516
520
39
393
410
279
298
513
201
501
419
171
295
318
427
28
272
259
0
66
443
145
254
242
228
407
372
93
382
33
252
15
505
182
449
113
423
70
445
157
477

Extended Data Figure 4. Times of greatest fractional species turnover in the Phanerozoic fossil record. Top 5% most significant proportionate extinction or origination times (corresponding to the 30 labelled and coloured times Fig. 3, > 42% species entry/exit threshold). “Drill plots” for focal times (key, top left) comparing stratigraphic ranges of all species occurring within 1 My of the focal time, vertically sorted into originations, extinctions and crossing ranges. Colours indicate over threshold mass extinctions (red), mass radiations (blue) and mixed mass extinction-radiations (magenta). Relevant stratigraphic unit names, dates and corresponding references are those used in the PBDB[30*, 31**,32].

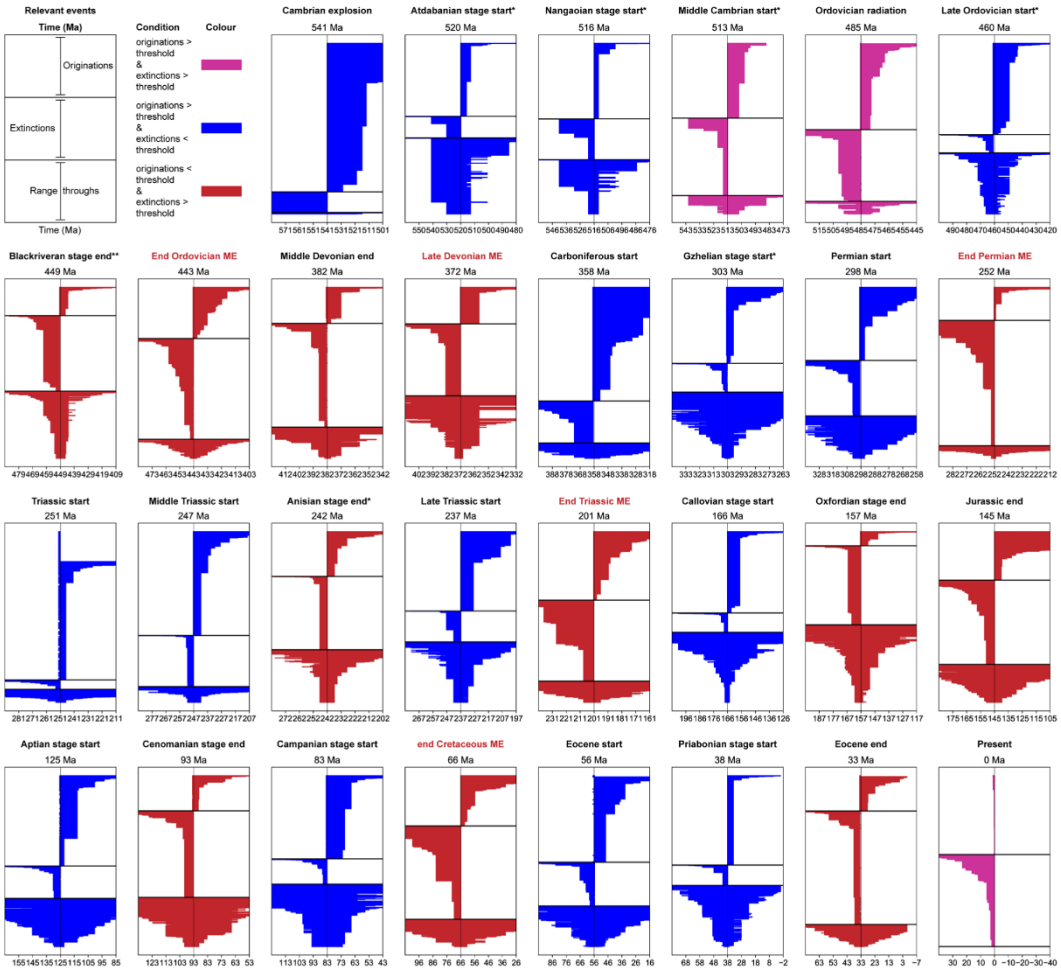
Relevant events
Time (Ma)
Originations
Extinctions
Range throughs
Time (Ma)
Condition
Colour
originations > threshold & extinctions > threshold
originations > threshold & extinctions < threshold
originations < threshold & extinctions > threshold
Cambrian explosion
541 Ma
Atdabanian stage start*
520 Ma
Nangaoian stage start*
516 Ma
Middle Cambrian start*
513 Ma
Ordovician radiation
485 Ma
Late Ordovician start*
460 Ma
Blackriveran stage end**
449 Ma
End Ordovician ME
443 Ma
Middle Devonian end
382 Ma
Late Devonian ME
372 Ma
Carboniferous start
358 Ma
Gzhelian stage start*
303 Ma
Permian start
298 Ma
End Permian ME
252 Ma
Triassic start
251 Ma
Middle Triassic start
247 Ma
Anisian stage end*
242 Ma
Late Triassic start
237 Ma
End Triassic ME
201 Ma
Callovian stage start
166 Ma
Oxfordian stage end
157 Ma
Jurassic end
145 Ma
Aptian stage start
125 Ma
Cenomanian stage end
93 Ma
Campanian stage start
83 Ma
end Cretaceous ME
66 Ma
Eocene start
56 Ma
Priabonian stage start
38 Ma
Eocene end
33 Ma
Present
0 Ma

Extended Data Figure 5. Breakdown by phylum of species extinctions and originations at the top 5% of evolutionary disruption times (corresponding to Fig. 3, Extended Data Fig. 4).

Proportions of species entering (dark blue) or exiting (dark red) the fossil record are shown for the 19 most prevalent phyla in the dataset (taxonomically screened dataset).

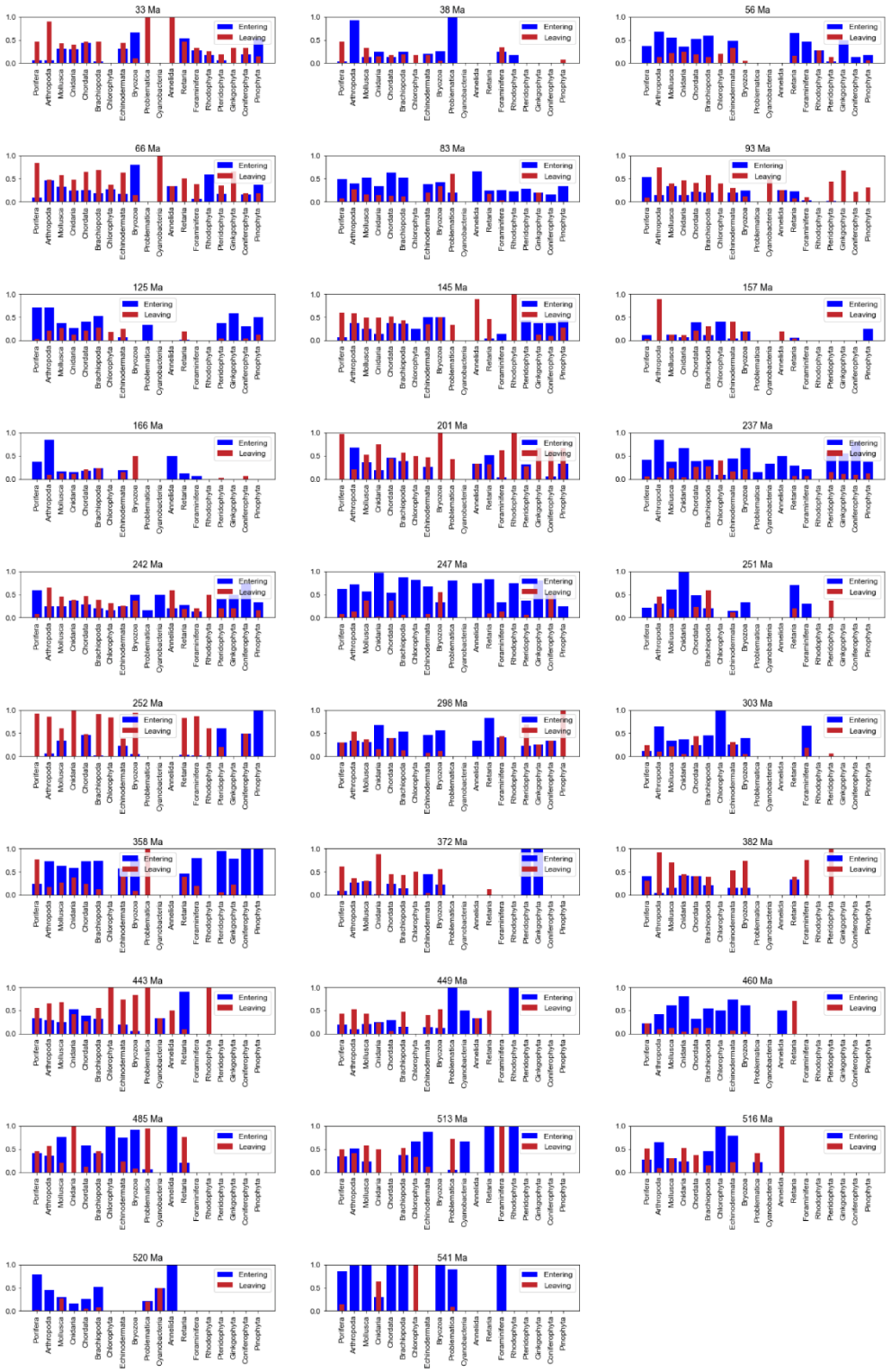
33 Ma
38 Ma
56 Ma
66 Ma
83 Ma
93 Ma
125 Ma
145 Ma
157 Ma
166 Ma
201 Ma
237 Ma
242 Ma
247 Ma
251 Ma
252 Ma
298 Ma
303 Ma
358 Ma
372 Ma
382 Ma
443 Ma
449 Ma
460 Ma
485 Ma
513 Ma
516 Ma
520 Ma
541 Ma
Entering
Leaving
1.0
0.5
0.0
Porifera
Arthropoda
Mollusca
Cnidaria
Chordata
Brachiopoda
Chlorophyta
Echinodermata
Bryozoa
Problematica
Cyanobacteria
Annelida
Retaria
Foraminifera
Rhodophyta
Pteridophyta
Ginkgophyta
Coniferophyta
Pinophyta

Extended Data Figure 6. a, Raw species time ranges. b, Raw diversity counts. c-f, Examples of the decay in probability of temporal co-occurrence. a, Time ranges (maximum occurrence – minimum occurrence) for 137,779 fossil species (taxonomically screened dataset). Taxonomically screened Phanerozoic dataset (535-0 Ma): median = 6.5 My, mean = 9.95 My, standard deviation = 12.86. Complete dataset: median 7 My, mean 14.4 standard deviation = 28.1 My. **b,** Sampled-in-bin taxonomic diversity of genera (grey dashed line) and families (black line) for the complete dataset, output by the PBDB within the default time bin of geological ages (at maximum Ma). **c-f,** Decay in co-occurrence probability (**c, e**) or shared fraction of species (**d, f**), from base times 1 My before versus after major evolutionary disturbance events. Grey dashed lines indicate a value of 0.1. **c, d,** End-Permian mass extinction at 252 Ma. **e, f,** Carboniferous mass radiation at 358 Ma. Following a disturbance event co-occurrence probabilities and shared fractions of species fall more rapidly to low levels as comparatively few living species co-occur with any species that were present in the past.

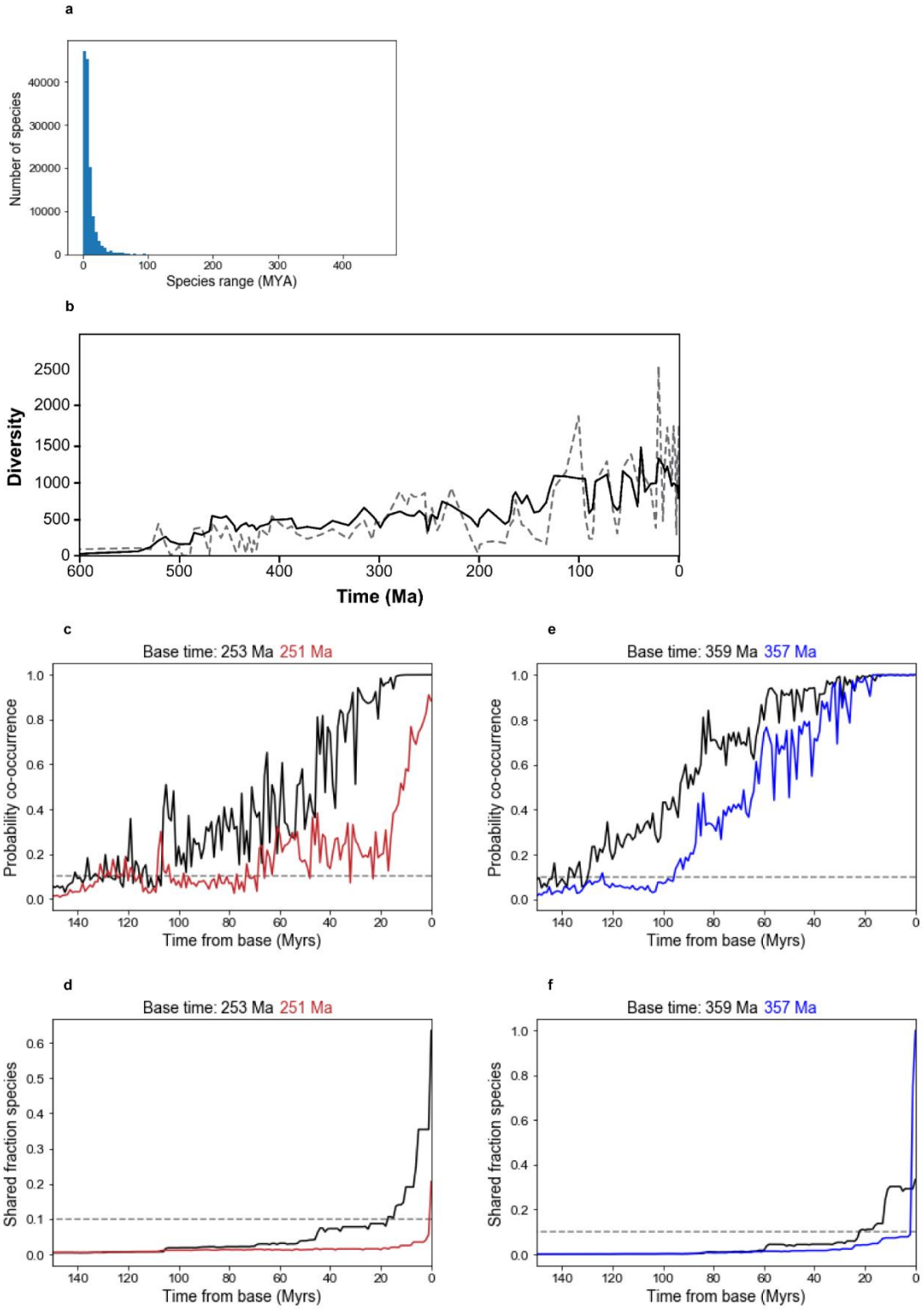
a
Number of species
40000
30000
20000
10000
0
0
100
200
300
400
Species range (MYA)
b
Diversity
2500
2000
1500
1000
500
0
600
500
400
300
200
100
0
Time (Ma)
c
Base time: 253 Ma 251 Ma
Probability co-occurrence
1.0
0.8
0.6
0.4
0.2
0.0
140
120
100
80
60
40
20
0
Time from base (Myrs)
e
Base time: 359 Ma 357 Ma
Probability co-occurrence
1.0
0.8
0.6
0.4
0.2
0.0
140
120
100
80
60
40
20
0
Time from base (Myrs)
d
Base time: 253 Ma 251 Ma
Shared fraction species
0.6
0.5
0.4
0.3
0.2
0.1
0.0
140
120
100
80
60
40
20
0
Time from base (Myrs)
f
Base time: 359 Ma 357 Ma
Shared fraction species
1.0
0.8
0.6
0.4
0.2
0.0
140
120
100
80
60
40
20
0
Time from base (Myrs)

Extended Data Figure 7. a-c, Conceptual diagram comparing measures of macroevolutionary decay. d, Decay-clock detail focussing on the last 40 million years. e. Statistical relationships between measures of macroevolutionary disturbance and time. a, Set representation of the shared fraction of species between compared times (e.g. times t1 and t2). This measure is used in this study and is closely conceptually related to the co-occurrence probability calculated using the ML spatial embedding (see methods for further details). **b,** Fraction of surviving species, a core concept of standard methods of survivor analysis e.g.[4]. These measures (**a, b**) will be equal if no new species have originated by time t2 (scenario **c**). Where new species have instead originated by time t2, their effect will be picked up by the measures used in this study (**a**) whereas the impact of new species would not be considered by measures only of the fraction of survivors from t1 (**b**). **d,** Vertical lines indicate times of evolutionary disturbance (blue, mass radiations; red mass extinctions, corresponding to Fig. 3, grey, turnover events below the mass-event threshold). **e,** 1. Measures of disturbance to co-occurrence structure calculated between consecutive time windows are largely independent of Phanerozoic time (over which there have been secular trends in raw diversity[20]). The shared fraction of species shows no significant relationship with time (taxonomically screened dataset). The embedding distance (complete dataset) shows a weak relationship across the whole Phanerozoic which is removed when Cenozoic data were excluded (data excluded in order to isolate hypothesised effect after initial data analysis), consistent with a weak effect on Cenozoic embedding distance from fossils with ranges extending to 0 Ma (which are particularly abundant in the dataset). 2. Proportions of species exiting or entering the fossil record within 1 million years of a given time show no significant relationship with time (taxonomically screened dataset). All statistical tests are two-tailed.

a

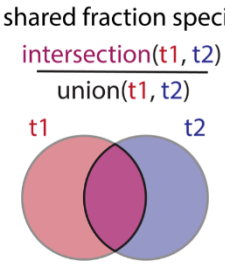

b

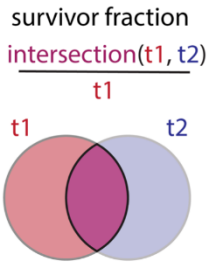

c

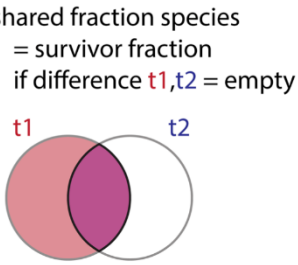

d

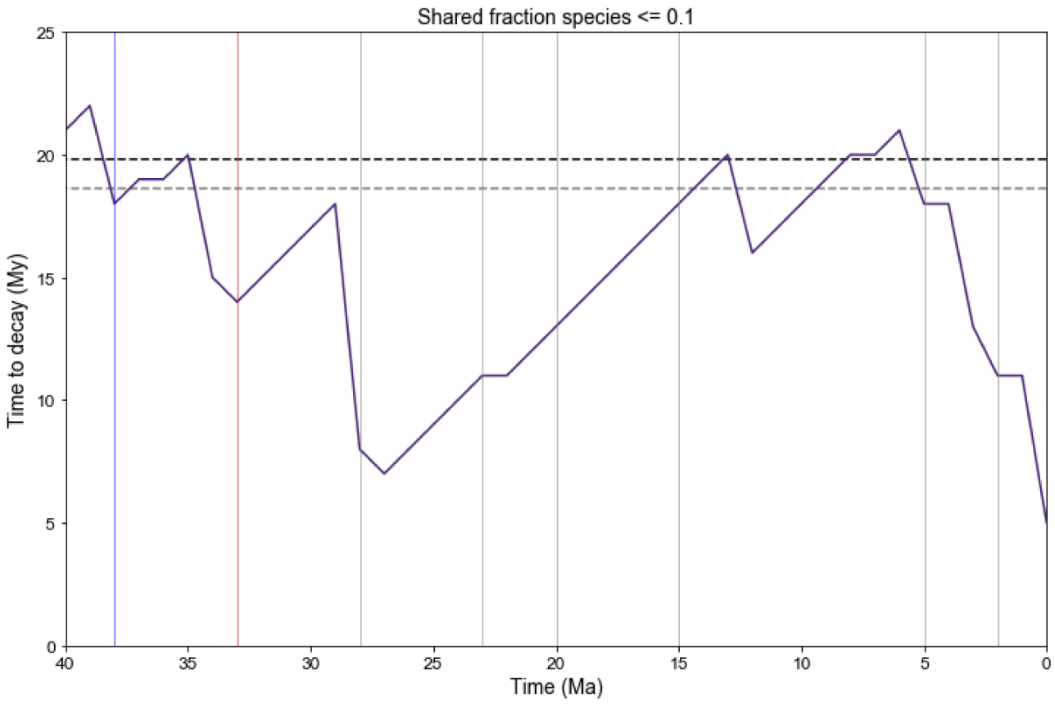

e

Measure	Sample size	Statistical test	Test statistic	Test statistic value	P value
Shared fraction species	532	Shapiro Wilk normality test	W	0.8117	1.94E-24
		Spearman nonparametric rank order correlation	r	0.054785	0.2071
Embedding distance	532	Shapiro Wilk normality test	W	0.9091	2.641E-17
		Spearman nonparametric rank order correlation	r	0.18554	1.6561E-05
Embedding distance 532-67 Ma	466	Spearman nonparametric rank order correlation	r	0.073272	0.1142
Fraction species going extinct	222	Shapiro Wilk normality test	W	0.8573	1.626E-13
		Spearman nonparametric rank order correlation	r	0.071236	0.29063
Fraction species originating	222	Shapiro Wilk normality test	W	0.8951	2.478E-11
		Spearman nonparametric rank order correlation	r	0.097941	0.1458